Published in final edited form as:
Langmuir. 2008 December 2; 24(23): 13614–13620. doi:10.1021/la802405p.

Pure Insulin Nanoparticle Agglomerates for Pulmonary Delivery

Mark M. Bailey[1], **Eric M. Gorman**[2], **Eric J. Munson**[2], and **Cory J. Berkland**[1,2,‡]

1 *Department of Chemical & Petroleum Engineering, University of Kansas, Lawrence, KS, USA 66047*

2 *Department of Pharmaceutical Chemistry, University of Kansas, Lawrence, KS, USA 66047*

Abstract

Diabetes is a set of diseases characterized by defects in insulin utilization, either through autoimmune destruction of insulin-producing cells (Type I) or insulin resistance (Type II). Treatment options can include regular injections of insulin, which can be painful and inconvenient, often leading to low patient compliance. To overcome this problem, novel formulations of insulin are being investigated, such as inhaled aerosols. Sufficient deposition of powder in the peripheral lung to maximize systemic absorption requires precise control over particle size and density, with particles between 1 and 5 μm in aerodynamic diameter being within the respirable range. Insulin nanoparticles were produced by titrating insulin dissolved at low pH up to the pI of the native protein, and were then further processed into microparticles using solvent displacement. Particle size, crystallinity, dissolution properties, structural stability, and bulk powder density were characterized. We have demonstrated that pure drug insulin microparticles can be produced from nanosuspensions with minimal processing steps without excipients, and with suitable properties for deposition in the peripheral lung.

Keywords

Insulin; Diabetes; Pulmonary Medicine; Crystallinity

INTRODUCTION

Diabetes mellitus is a set of diseases characterized by defects in insulin utilization, either from autoimmune destruction of insulin-producing cells (Type I) or insulin resistance (Type II). As of 2005, 20.8 million people in the United States (7.0% of the population) suffered from diabetes, and it was the sixth leading cause of death due to the many complications associated with this disease, such as pulmonary hypertension and ischemia.[1] Current treatment methods involve regular injections of insulin, which can be both painful and inconvenient, thus often leading to low patient compliance.[2]

In order to overcome this problem, other routes of insulin administration have been investigated. Inhaled aerosols have been shown to be an effective means to treat local diseases of the lung.[3] Additionally, the large surface area of the lungs (~140 m^2) and their ready access to systemic circulation makes them a possible candidate for noninvasive, systemic drug delivery. This is particularly good for macromolecular drugs such as peptides, proteins, and DNA.[3–5]

Sufficient deposition of aerosol particles in the peripheral lung requires precise control over particle size and density, which greatly affect the region of deposition in the lungs.[4–9] Particles

‡Corresponding Author: Address: 2030 Becker Drive, Lawrence, KS 66047; Telephone: 785-864-1455; Fax: 785-864-1454; Email: berkland@ku.edu.

possessing an aerodynamic diameter in the range of 1–5 μm are required for suitable terminal bronchiole and alveolar deposition,[6, 8–10] as a means to access systemic bioavailability.[7] Low-density particles are currently being developed as a means to deliver drugs to the distal regions of the lungs.[5, 7, 11, 12] These particles possess large geometric diameters, but smaller aerodynamic diameters due to their low density, as described by the following equation,[6, 8, 13]

$$d_{aero}=d_{geo}\left[\frac{\left(\rho/\rho_{ref}\right)}{\gamma}\right]^{0.5} \quad [1]$$

Where ρ_{ref} is a reference density (for example 1 g/cm^3) and γ is the shape factor (equal to 1 for a sphere).

Studies have shown that insulin delivered via the pulmonary route is well tolerated and effective in treating patients with Type I diabetes.[10, 12, 14–19] Currently, there are several inhaled insulin delivery systems in development. Of these, those employing the Technosphere (Mannkind Corporation) and Spiros technologies (Dura Pharmaceuticals) are dry powder formulations.[14] The Exubera formulation (Nektar Therapeutics and Pfizer) and the formulation using AIR technology (Alkermes and Eli Lilly) are other examples of dry powder formulations that were either FDA approved and discontinued (Exubera), or terminated during Phase III clinical trials (AIR). One potential drawback to these formulations is that they contain excipients, which aid in manufacturing and aerosol performance, but may have unforeseen negative impacts on the long-term respiratory health of the patient.[2, 17] Of particular concern are penetration enhancers, such as polyoxyethylene 9 lauryl ether and sodium glycocholate, which have been shown to induce acute inflammation in the lung.[20] It may therefore be desirable to create an inhalable form of insulin that does not contain excipients so as to avoid any potential complications that might arise. Additionally, most of the current technologies use a spray drying technique to produce particles, which can subject the insulin to air/water interfaces, high temperatures, and other conditions that can cause the protein to denature.

Here, a dry powder Zn-insulin formulation possessing appropriate microstructure to reach the deep lung that is processed without excipients has been developed using a “bottom-up” approach (Figure 1). Factors such as pH and insulin concentration were shown to have an affect on seed nanoparticle size. Circular dichroism (CD) and solid-state nuclear magnetic resonance (ssNMR) were used to show that irreversible secondary structure and crystallinity changes of the insulin did not occur as a result of processing. It has been demonstrated that excipient-free, insulin microparticles that are suitably sized for pulmonary delivery and have a high dissolution velocity can be produced with minimal processing steps. This approach to insulin powder formulation development may help future researchers develop novel pulmonary delivery systems for the treatment of diabetes, and as a general approach to formulate small peptides as nanoparticles or microparticles without the use of excipients

MATERIALS AND METHODS

1. Materials

Lyophilized insulin powder from bovine pancreas (0.5% zinc content) and phosphate buffered saline premix (PBS) were purchased from Sigma (St. Louis, MO). All other reagents were purchased from Fisher Scientific (Pittsburgh, PA) and used without further purification.

2. Fabrication of insulin nanoparticles

Approximately 100 mg of insulin stock powder were dissolved in 15 mL of 0.01 N HCl solution. The solution was then titrated drop-wise to a pH just below the isoelectric point (pI) of the native protein (5.3) with 0.01 N NaOH solution, at which point the solution became colloidal without precipitating. The mean geometric diameters and polydispersities of the nanoparticle suspension were measured using dynamic light scattering (Brookhaven Instruments Zeta Potential Analyzer, Holtsville, NY). Nanoparticles were diluted in deionized H_2O (~100X) and three, 1 minute measurements were obtained at 25°C for each sample. Mean size and polydisperity were determined by the method of cumulants.[21] The same instrument was used to determine the zeta potential (ζ) of the nanoparticles in 1 mM potassium chloride solution. Three runs of 15 cycles were acquired, and the mean zeta potential was recorded. Some samples were frozen at −80°C and lyophilized using a Labconco bench top lyophilizer (Kansas City, MO) for further analysis.

A range of pH values near the pI of the native protein were determined in which the nanoparticle colloid was preserved. Particle sizes and zeta potentials were measured for each sample. Nanoparticle samples within this pH range (from 4.92 to 5.09) were centrifuged at 13,000 rpm for 10 minutes and the supernatant concentration of insulin was analyzed using UV absorbance spectroscopy (Agilent 8453). All pH values were measured in triplicate. The measured concentration was used to calculate the mass of insulin in the pellet from the original insulin mass and total volume.

3. Agglomeration of insulin microparticles

5 mL aliquots of insulin nanoparticle suspensions were added to 15 mL of ethanol and stirred for ~36 hours at 300 rpm under a fume hood. Nanoparticles with diameters of approximately 200 nm were selected for this step. The geometric diameters of the insulin microparticles were measured in Isoton™ diluent using a Coulter Multisizer™ 3 (Beckman Coulter, Fullerton, CA). Samples were frozen at −80 °C and lyophilized for further analysis.

4. Characterization of aerosol properties

The aerodynamic diameters of the lyophilized powders were determined using an Aerosizer LD (Amherst Process Instruments Inc.). Data were collected over ~70 seconds under high shear force (~3.4 kPa) using a 700 μm nozzle.

5. Characterization of particle morphology

The size and morphology of lyophilized samples were evaluated using a LEO 1550 field emission scanning electron microscope (SEM). All samples were sputter-coated with gold for 30 seconds prior to imaging.

6. Conformational stability of processed insulin

Post-processing secondary structural changes in samples were analyzed by dissolving particles in 0.01 N HCl solution and subjection to circular dichroism spectroscopy (CD; Jasco J-810, Easton, MD) to determine conformational differences between processed and unprocessed insulin, as well as thermal stability differences between groups. CD spectra were acquired in three accumulations from 260-195 nm with a scanning speed of 50 nm/min and 1.0 nm resolution. Thermal stability was determined at a wavelength of 210 nm from 10–80 °C with a scanning speed of 15 °C/hr. Thermal stability spectra were acquired in triplicate. Insulin concentration in prepared solutions was determined by UV absorbance spectroscopy.

7. Crystallinity of processed insulin

7.1. NMR—Spectra were collected using a Tecmag Apollo spectrometer operating at 300 MHz using ramped amplitude cross-polarization (RAMP),[22] magic-angle spinning (MAS),[23] and SPINAL-64 decoupling.[24] Samples were packed in 4 mm o.d. zirconia rotors using Teflon® endcaps, and spun at 8 kHz in a ChemagneticsTM Triple-Resonance HXY CP/MAS NMR probe configured to run in double-resonance mode using the H and X channels, and fitted with a 4 mm spin module from Revolution NMR. All spectra are the sum of 120,000 transients collected using a 1.5 s pulse delay, a contact time of 2 ms, and a 1H 90° pulse width of 2.3 μs. The free induction decays consisted of 256 points with a dwell time of 33.3 μs. The spectra were externally referenced to tetramethylsilane using the methyl peak of 3-methylglutaric acid at 18.84 ppm.[25]

7.2 HPLC—The crystalline insulin content of the materials was determined using the method in the insulin-zinc suspension monograph of the 2005 U.S. Pharmacopoeia National Formulary, with minor modifications. Buffered acetone TS was produced by dissolving 8.15 g of sodium acetate and 42 g of sodium chloride in 100 mL of water, to which 68 mL of 0.1 N hydrochloric acid and 150 mL of acetone were added. The mixture was then diluted with water to make 500 mL. Approximately 0.5 mg of insulin was placed in a 1.5 mL microcentrifuge tube and 33.3 μL of a 1:2 mixture of water and buffered acetone TS was added to the tube to extract any amorphous insulin. The sample was immediately centrifuged at 13,000 rpm for one minute, the supernatant was decanted, and the extraction was repeated. Additionally, ~0.5 mg of insulin was placed in another microcentrifuge tube to be used as a control. Both insulin samples were each dissolved in 33.3 μL of 0.01 N hydrochloric acid and analyzed by HPLC, with each sample being prepared in triplicate.

The HPLC was a Shimadzu system that consisted of an SCL-10A system controller, LC-10AT liquid chromatography pump, SIL-10A auto injector with a sample cooler, and SPD-10A UV-VIS detector with instrument control and data analysis performed through CLASS-VP software. Aqueous mobile phase was prepared by dissolving 28.4 g of anhydrous sodium sulfate in 1000 mL of water, to which 2.7 mL of phosphoric acid was added and the pH was adjusted to 2.3 with ethanolamine. The aqueous mobile phase was then mixed 74:26 with acetonitrile. The separation was performed on a 4.6 × 250 mm Symmetry® C18 column from Waters that was maintained at 40°C. Samples were maintained at 5°C and 20 μL were injected for analysis, with a mobile phase flow rate of 1 mL/min and the detector set to 215 nm. Peak areas were normalized to the mass of insulin used to prepare the sample and the percent crystalline insulin was calculated with the following equation:

$$\%Crystalline = \frac{SamplePeak}{ControlPeak} \times 100 \quad [2]$$

8. Dissolution of insulin particles

Approximately 6 mg of each insulin particle sample was suspended in PBS (pH 7.4). The solution was placed in a 100,000 Dalton biotech grade cellulose ester dialysis tube (Spectrum Labs, Rancho Dominiguez, CA) and placed in PBS solution to a final volume of 45 mL. All samples were incubated at 37°C and shaken at 50 rpm on a shaker table. One mL aliquots were taken at various time points up to 8 hours from the bulk solution and replaced with 1 mL of fresh PBS. The insulin concentration was measured using a Coomassie Plus colorimetric protein quantification assay (Thermo Fisher Scientific, Waltham, MA). A calibration curve was used to correlate the insulin concentration with the measured absorbance, with insulin concentrations ranging between 1 and 25 μg/mL being used as the standard. Dissolved mass was calculated from the measured concentration, and was then normalized to the total loaded

mass to determine the percent dissolved. All experiments were performed in triplicate. Analysis of variance (ANOVA) was used to determine statistically significant differences between groups ($p < 0.05$). Comparisons among groups were done using a Fisher's *F*-test. Data points were fit to a variation of the Hguchi Equation (Equation 2) by minimizing the sum of the squared residuals.

$$x = k \cdot t^{1/2} \quad [2]$$

Where x is the fraction released, t is the time elapsed, and k is a constant. A t-test was used to show the correlation between the experimental data and the model.

9. Estimation of bulk powder density

The bulk density of the dry powder was estimated using a micro-tap test approach, as defined in the U.S. Pharmacopoeia National Formulary, with slight modifications. Briefly, dry powder samples (unprocessed insulin, nanoparticles, and microparticles) were added to pre-weighed microcentrifuge tubes, and the tubes were weighed again to determine the mass of powder. The tubes were then tapped thirty times on the lab bench to compress the powder. The volume of the powder was approximated by comparing the height of the compressed powder to that of a volume of water in an identical pre-weighed microcentrifuge tube. The tube containing the water was then weighed to determine the volume of water (assuming a density of 1 g/cm^3). The powder density was calculated by dividing the mass of powder by the volume of water. All samples were analyzed in triplicate. Analysis of variance (ANOVA) was used to determine statistically significant differences between groups ($p < 0.05$). Comparisons among groups were done using a Fisher's *F*-test.

RESULTS

1. Characterization of insulin nanoparticles

Zinc-insulin nanoparticles were created by titrating dissolved insulin to the pI of the native protein, which resulted in a colloidal suspension of nanoparticles. Particle sizes and zeta potentials were analyzed over a pH range of 4.9 to 5.1, and ranged from 293 nm to 592 nm (Table I). Zeta potentials ranged from 10.9 mV to 18.9 mV. Neither particle sizes nor zeta potentials correlated strongly with the pH of the solution.

The mass fraction of insulin remaining in solution after nanoparticle precipitation was determined using UV absorbance spectroscopy. These values were used to determine the mass fraction of total insulin contained in the nanoparticles. The results suggest a positive correlation between the particle size and the total mass of the insulin nanoparticles in suspension (Figure 2), which corroborates the increase in particle size with increasing pH as shown in Table I.

2. Characterization of insulin microparticles

Insulin microparticles were produced from insulin nanoparticle suspensions through solvent displacement. This was achieved by adding aliquots of insulin nanoparticle suspension to ethanol and stirring for 36 hours. The geometric diameter of the insulin microparticles was determined to be 3.41 ± 1.4 μm. No correlation was determined to exist between insulin nanoparticle size and microparticle size (Figure 3). SEM imaging revealed differences in the morphology of the unprocessed insulin and the insulin microparticles (Figure 4). The unprocessed insulin appears as agglomerates of micronized zinc-insulin crystals, while the microparticles have a more leaf-like morphology. This leaf-like shape could aid in the

aerosolizability of the insulin microparticles, and would suggest a shape factor (as defined in Equation 1) of much less than 1.

3. Bulk powder density

The tap test method was used to determine the bulk density of the insulin powders before and after processing. Density of the unprocessed insulin powder was determined to be 0.48 ± 0.08 mg/cm^3 (Figure 5). The nanoparticle bulk density was determined to be 0.28 ± 0.04 mg/cm^3, and the bulk density of the insulin microparticles was determined to be 0.063 ± 0.004 mg/cm^3. Analysis of variance revealed a p-value of 0.00025 ($p < 0.05$), indicating a statistically significant difference between the bulk densities of each group.

4. Aerosol properties - insulin particles

The aerodynamic diameters of the unprocessed insulin powder, lyophilized insulin nanoparticles, and lyophilized insulin microparticles were measured with an Aerosizer LD and are shown in Table II. The large aerodynamic diameter of the insulin nanoparticles is most likely due to uncontrolled agglomeration, which probably occurred during lyophilization. The smaller aerodynamic diameter of the insulin microparticles compared to the geometric diameter (see Supplementary Figure 1) of the microparticles was expected because of the lower density and morphology of the insulin microparticles (Figure 5).

5. Conformational stability of processed insulin

Circular dichroism (CD) was employed to analyze the secondary structure and thermal stability of processed insulin powders. Isothermal scans of dissolved, unprocessed insulin powder, dissolved nanoparticles, and dissolved microparticles reveal near-identical spectra with minima at 210 nm, suggesting that there were no changes in the secondary structure of processed insulin (Figure 6). Retention of secondary structure was also reflected in the thermal stability CD scans, which showed a slight change in molar ellipticity starting at about 50°C for all samples. Data are indicative of a loss of secondary structure occurring at the same melting temperature for all insulin samples. The data suggest that there were no changes that occurred as a result of processing, and that the thermal stability of the insulin processed into microparticles and nanoparticles was neither enhanced nor diminished.

6. Crystallinity of processed insulin

The crystallinity of the insulin particles was examined using 13C CP/MAS NMR (Figure 7). The spectra displayed differences in the aliphatic region (~0 to 75 ppm), although these differences are difficult to correlate with the physical state of insulin. More obvious differences between the samples existed in the carbonyl (~175 ppm) and aromatic (~137 ppm) regions. The peak at ~137 ppm in the unprocessed insulin seemed to be more narrow and better resolved than peaks at ~129 ppm. These same lines in the other samples were broader, to the point where peaks at ~129 ppm could not be resolved. The peak at ~175 ppm in the unprocessed insulin was more narrow, with two very clear shoulders at ~180 ppm and ~173 ppm. Other samples only showed one broad peak at ~175 ppm.

7. Dissolution of insulin particles

The concentration of insulin was measured over time in PBS to determine the dissolution rate of the different powders (Figure 8). The unprocessed insulin follows Higuchi dissolution kinetics,[26] where the amount of drug released is proportional to the square root of time (Equation 2). The nanoparticles and microparticles appear to show a burst dissolution phenomenon, but follow a similar release pattern. A statistically significant fit was determined to exist between the model and the experimental data ($p = 2 \times 10^{-7}$, $p = 0.00003$, and $p = 0.00007$ for unprocessed, nanoparticles, and microparticles, respectively). The final

concentrations of dissolved nanoparticles and microparticles were both significantly different from that of unprocessed powder after 15 minutes ($p = 0.0021$ and $p = 0.0054$, respectively). The dissolution rates of neither the nanoparticles nor the microparticles were significantly different from the dissolution rate of the unprocessed insulin after 8 hours.

DISCUSSION

Pure insulin microparticles with sizes within the respirable range were produced from the solvent displacement from insulin nanoparticles. Nanoparticles were produced using titration and were shown to have a strong correlation between pH and particle size (Figure 2). Microparticles were then produced using ethanol to displace the aqueous solvent and induce nanoparticle agglomeration. The resulting microparticles showed a “leaf-like” (flat, thin and curled) morphology. The proposed mechanism for this agglomeration is a combination of decreased electrostatic interactions between nanoparticles due to the addition of the organic phase, and the deposition of dissolved insulin onto the surface of the nanoparticles as the solubility of the insulin is reduced. It might be possible that the addition of the organic phase caused an increased hydrophobic interaction between the particles as hydrophobic amino acid residues of the insulin extended into the organic solvent, causing particle cohesion and coalescence. Future studies should aim to understand this mechanism of nucleation and growth in greater detail.

The sizes of the microparticles were independent of the size of the nanoparticles used, and had a mean aerodynamic diameter that was roughly between 0.4 μm and 4 μm, with a mean diameter of 2.3 μm. This range of average particle sizes is similar to other dry powder insulin formulations, such as Exubera (3.5 μm),[18] and a formulation based on the Spiros technology (2–3 μm).[27] Additionally, these particles were smaller than those produced using AIR technology (5–30 μm).[28] Based on Equation 1, our data suggest a mean shape factor equal to 0.135 (assuming a ρ_{ref} of 1 mg/cm^3 and $\rho_{tap} = \rho_{particle}$). This value is much less than 1, indicating that our particles are aspherical and highly irregular in morphology, potentially making them good candidates for inhalation. This observation was further corroborated by SEM imaging (Figure 4).

The crystallinity of the insulin particles was first examined using 13C CP/MAS NMR (Figure 7). Due to their highly ordered nature, crystalline materials have relatively narrow lines in a 13C CP/MAS spectrum, while disordered or amorphous materials have relatively broad lines. Insulin consists of 51 amino acids and therefore the spectrum will be quite complicated because every amino acid will have at least an amide and a carbon, each of which will have slightly different conformations and thus different chemical shifts. Because of this, even the 13C CP/MAS spectrum of a crystalline protein would appear to have broad lines even though it consists of many narrow lines with slightly different chemical shifts. Therefore, it would be expected that there would be very few differences between the 13C CP/MAS spectra of amorphous and crystalline proteins, and any differences may be subtle. The sharply resolved peaks of the unprocessed insulin suggested that it is crystalline while spectra for all other samples suggested some amorphous content, which is corroborated by the dissolution testing. However, at this time nothing can be said about the purity of each form because some crystalline insulin may exist in samples that appear to be amorphous.

Crystallinity was also determined by dissolution testing, as defined by the 2005 U.S. Pharmacopoeia National Formulary, with modifications. Buffered acetone was used to dissolve the amorphous insulin from each sample, the concentration of which was then determined and used to estimate the crystallinity of the particles. The unprocessed insulin (~85% crystalline) was shown to be about 17 times more crystalline than the nanoparticles, and 4 times more crystalline than the microparticles (Figure 9). In addition, the dissolution rate of both the

microparticles and the nanoparticles exhibited a burst effect over the first few minutes when compared to the unprocessed insulin (Figure 8). This is indicated because the nanoparticle and microparticle dissolution data do not fit to the model at the shortest times. This burst may be due to the rapid dissolution of amorphous material deposited on the surface of the particles during processing or possibly during lyophilization. In the case of the nanoparticles, it is probable that the large total surface area of the particles also plays a significant role in increasing the dissolution rate. This may be beneficial in a pulmonary insulin formulation if the desired therapeutic effect is rapid control of spikes in glucose levels.

A concern with the technique outlined in the U.S. Pharmacopoeia is that it is based on the assumption that amorphous materials dissolve more rapidly than crystalline materials. This assumption might not always apply when using nanoparticles because of the enhanced dissolution velocity of particles at this scale, so interpretation of the results should be approached conservatively.[29, 30] Additionally, future studies should aim to examine the shelf-life of the formulation using an accelerated stability study. Solid-state drug formulations can be more thermodynamically stable in their crystalline forms than in their amorphous forms, transitions of amorphous insulin to crystalline could cause the microparticle formulation to lose its burst-release properties over time, if indeed the burst dissolution is the result of amorphous content as opposed to nanostructure. Future studies should also include examination of the formulation *in vivo* to determine the relative performance of this formulation over intravenous and subcutaneous insulin formulations, as well as other pulmonary insulin formulations.

CONCLUSIONS

Pure insulin microparticles produced through agglomeration of insulin nanoparticles may be a potential candidate for a pulmonary insulin formulation. The lack of penetration enhancers and other excipients in this formulation may reduce the occurrence of unforeseen side effects, thus making it potentially safer than existing alternatives. Additionally, the processing steps necessary for this formulation are minimal and did not denature or degrade the peptide, which may be a concern with currently used techniques. A major benefit of this formulation method is the ability to produce pure insulin microparticles, which has not been demonstrated with techniques such as spray drying. The development of a dry powder insulin formulation for the treatment of diabetes may help to reduce, or altogether eliminate, patient dependence on painful injections, and thus may help to increase patient compliance.

Supplementary Material

Refer to Web version on PubMed Central for supplementary material.

Acknowledgements

The authors would like to acknowledge funding from the Cystic Fibrosis Foundation, the NIH (R03 AR054035, P20 RR016443 and P20 RR015563), the American Heart Association, the Coulter Foundation, and support from the Madison and Lila Self Graduate Fellowship at the University of Kansas. The authors graciously acknowledge Professor C. Russell Middaugh for use of his equipment, and Dr. David Moore and Heather Shinogle from the Microscopy & Analytical Imaging Lab at the University of Kansas for their assistance.

References

1. National Diabetes Fact Sheet: General Information and National Estimates on Diabetes in the United States. U.S. Department of Health and Human Services, Centers for Disease Control and Prevention; Atlanta, GA: 2005.

2. Kwon JH, Lee BH, Lee JJ, Kim CW. Insulin microcrystal suspension as a long-acting formulation for pulmonary delivery. Eur J Pharm Sci 2004;22(2–3):107–16. [PubMed: 15158896]
3. Happel KI, Lockhart EA, Mason CM, Porretta E, Keoshkerian E, Odden AR, Nelson S, Ramsay AJ. Pulmonary interleukin-23 gene delivery increases local T-cell immunity and controls growth of Mycobacterium tuberculosis in the lungs. Infect Immun 2005;73(9):5782–8. [PubMed: 16113296]
4. Fuso L, Pitocco D, Incalzi RA. Inhaled insulin and the lung. Curr Med Chem 2007;14(12):1335–47. [PubMed: 17504216]
5. Patton JS. Pulmonary delivery of drugs for bone disorders. Adv Drug Deliv Rev 2000;42(3):239–48. [PubMed: 10963838]
6. Edwards DA, Ben-Jebria A, Langer R. Recent advances in pulmonary drug delivery using large, porous inhaled particles. J Appl Physiol 1998;85(2):379–85. [PubMed: 9688708]
7. Edwards DA, Hanes J, Caponetti G, Hrkach J, Ben-Jebria A, Eskew ML, Mintzes J, Deaver D, Lotan N, Langer R. Large porous particles for pulmonary drug delivery. Science 1997;276(5320):1868–71. [PubMed: 9188534]
8. Musante CJ, Schroeter JD, Rosati JA, Crowder TM, Hickey AJ, Martonen TB. Factors affecting the deposition of inhaled porous drug particles. J Pharm Sci 2002;91(7):1590–600. [PubMed: 12115821]
9. Newman SP. Drug delivery to the lungs from dry powder inhalers. Curr Opin Pulm Med 2003;9(Suppl 1):S17–20. [PubMed: 12974538]
10. Hegewald M, Crapo RO, Jensen RL. Pulmonary function changes related to acute and chronic administration of inhaled insulin. Diabetes Technol Ther 2007;9(Suppl 1):S93–S101. [PubMed: 17563309]
11. Arnold MM, Gorman EM, Schieber LJ, Munson EJ, Berkland C. NanoCipro encapsulation in monodisperse large porous PLGA microparticles. J Control Release 2007;121(1–2):100–9. [PubMed: 17604870]
12. Wollmer P, Pieber TR, Gall MA, Brunton S. Delivering needle-free insulin using AERx iDMS (insulin diabetes management system) technology. Diabetes Technol Ther 2007;9(Suppl 1):S57–64. [PubMed: 17563305]
13. Shi L, Plumley CJ, Berkland C. Biodegradable nanoparticle flocculates for dry powder aerosol formulation. Langmuir 2007;23(22):10897–901. [PubMed: 17894513]
14. Bellary S, Barnett AH. Inhaled insulin (Exubera): Combining efficacy and convenience. Diab Vasc Dis Res 2006;3(3):179–85. [PubMed: 17160913]
15. Cefalu WT, Wang ZQ. Clinical research observations with use of exubera in patients with type 1 and 2 diabetes. Diabetes Technol Ther 2007;9(Suppl 1):S28–40. [PubMed: 17563301]
16. Dailey G. Developing a pulmonary insulin delivery system for patients with diabetes. Clin Ther 2007;29:1271–83.Spec No
17. de Galan BE, Simsek S, Tack CJ, Heine RJ. Efficacy and safety of inhaled insulin in the treatment of diabetes mellitus. Neth J Med 2006;64(9):319–25. [PubMed: 17057268]
18. Harper NJ, Gray S, De Groot J, Parker JM, Sadrzadeh N, Schuler C, Schumacher JD, Seshadri S, Smith AE, Steeno GS, Stevenson CL, Taniere R, Wang M, Bennett DB. The design and performance of the exubera pulmonary insulin delivery system. Diabetes Technol Ther 2007;9(Suppl 1):S16–27. [PubMed: 17563300]
19. Norwood P, Dumas R, Cefalu W, Yale JF, England R, Riese R, Teeter J. Randomized study to characterize glycemic control and short-term pulmonary function in patients with type 1 diabetes receiving inhaled human insulin (exubera). J Clin Endocrinol Metab 2007;92(6):2211–4. [PubMed: 17003088]
20. Suzuki M, Machida M, Adachi K, Otabe K, Sugimoto T, Hayashi M, Awazu S. Histopathological study of the effects of a single intratracheal instillation of surface active agents on lung in rats. J Toxicol Sci 2000;25(1):49–55. [PubMed: 10736790]
21. Koppel DE. Analysis of Macromolecular Polydispersity in Intensity Correlation Spectroscopy: The Method of Cumulants. The Journal of Chemical Physics 1972;57(11):4814–4820.
22. Metz G, Wu XL, Smith SO. Ramped-Amplitude Cross Polarization in Magic-Angle-Spinning NMR. Journal of Magnetic Resonance, Series A 1994;110(2):219–227.
23. Stejskal EO, Schaefer J, Waugh JS. Magic-angle spinning and polarization transfer in proton-enhanced NMR. Journal of Magnetic Resonance (1969) 1977;28(1):105–112.

24. Fung BM, Khitrin AK, Ermolaev K. An improved broadband decoupling sequence for liquid crystals and solids. J Magn Reson 2000;142(1):97–101. [PubMed: 10617439]

25. Barich DH, Gorman EM, Zell MT, Munson EJ. 3-Methylglutaric acid as a 13C solid-state NMR standard. Solid State Nuclear Magnetic Resonance 2006;30(3–4):125–129. [PubMed: 16887343]

26. Higuchi T. Mechanism of Sustained-Action Medication. Theoretical Analysis of Rate of Release of Solid Drugs Dispersed in Solid Matrices. J Pharm Sci 1963;52:1145–9. [PubMed: 14088963]

27. Rave K, Nosek L, Heinemann L, Gonzales C, Ernest CS, Chien J, Muchmore D. Inhaled micronized crystalline human insulin using a dry powder inhaler: dose-response and time-action profiles. Diabet Med 2004;21(7):763–8. [PubMed: 15209771]

28. Cefalu WT. Concept, strategies, and feasibility of noninvasive insulin delivery. Diabetes Care 2004;27 (1):239–46. [PubMed: 14693996]

29. Lindfors L, Skantze P, Skantze U, Rasmusson M, Zackrisson A, Olsson U. Amorphous drug nanosuspensions. 1. Inhibition of Ostwald ripening. Langmuir 2006;22(3):906–10. [PubMed: 16430247]

30. Lindfors L, Skantze P, Skantze U, Westergren J, Olsson U. Amorphous drug nanosuspensions. 3. Particle dissolution and crystal growth. Langmuir 2007;23(19):9866–74. [PubMed: 17696457]

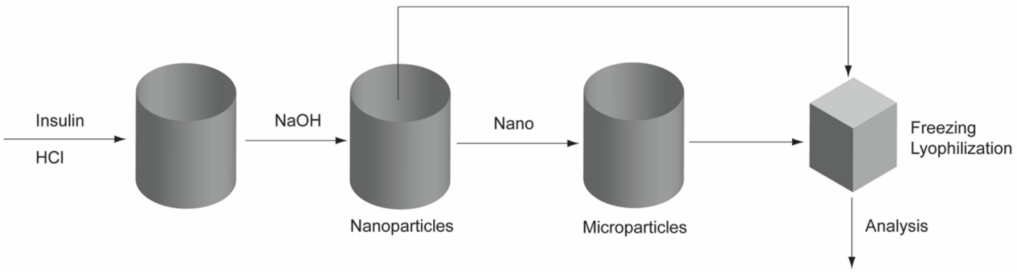

Figure 1.
Outline of insulin processing method showing the different processing steps. “Nano” refers to insulin nanoparticles, which were processed into microparticles.

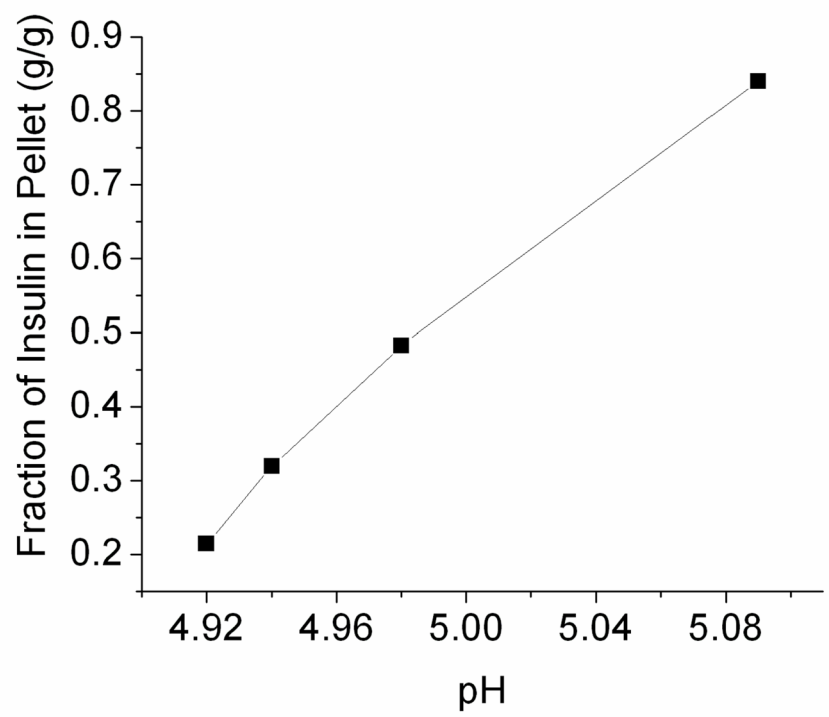

Figure 2.
Mass fraction of insulin in pellet vs. pH. Pellet mass increased as pH increased as insulin precipitated out of solution. Each value represents the mean ± S.D. of three experiments.

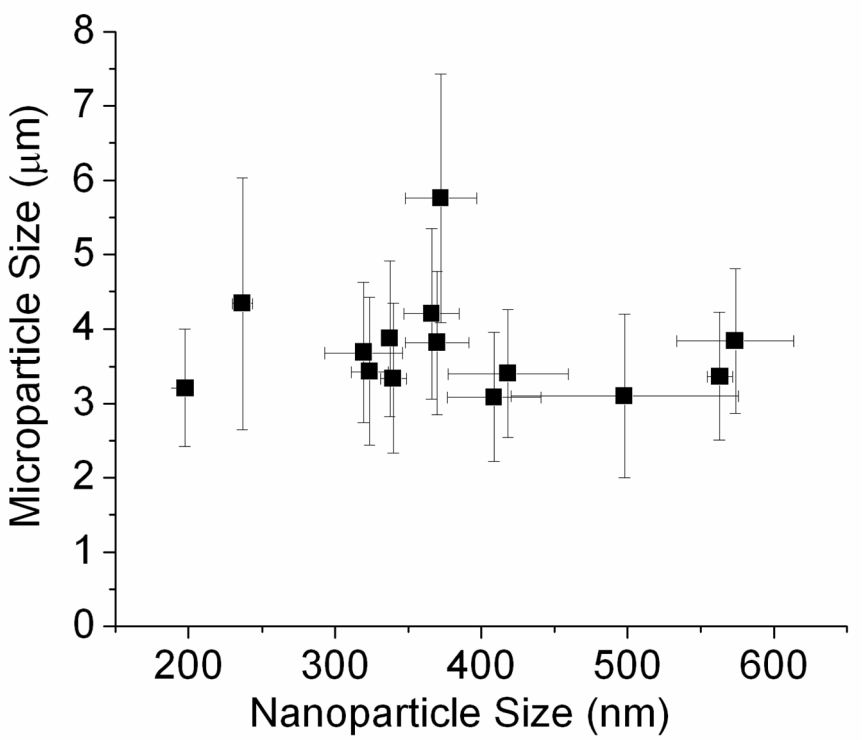

Figure 3.
Microparticle size vs. nanoparticle size. Data suggest no correlation between nanoparticle size and microparticle size. Each point represents the mean ± S.D. of three experiments.

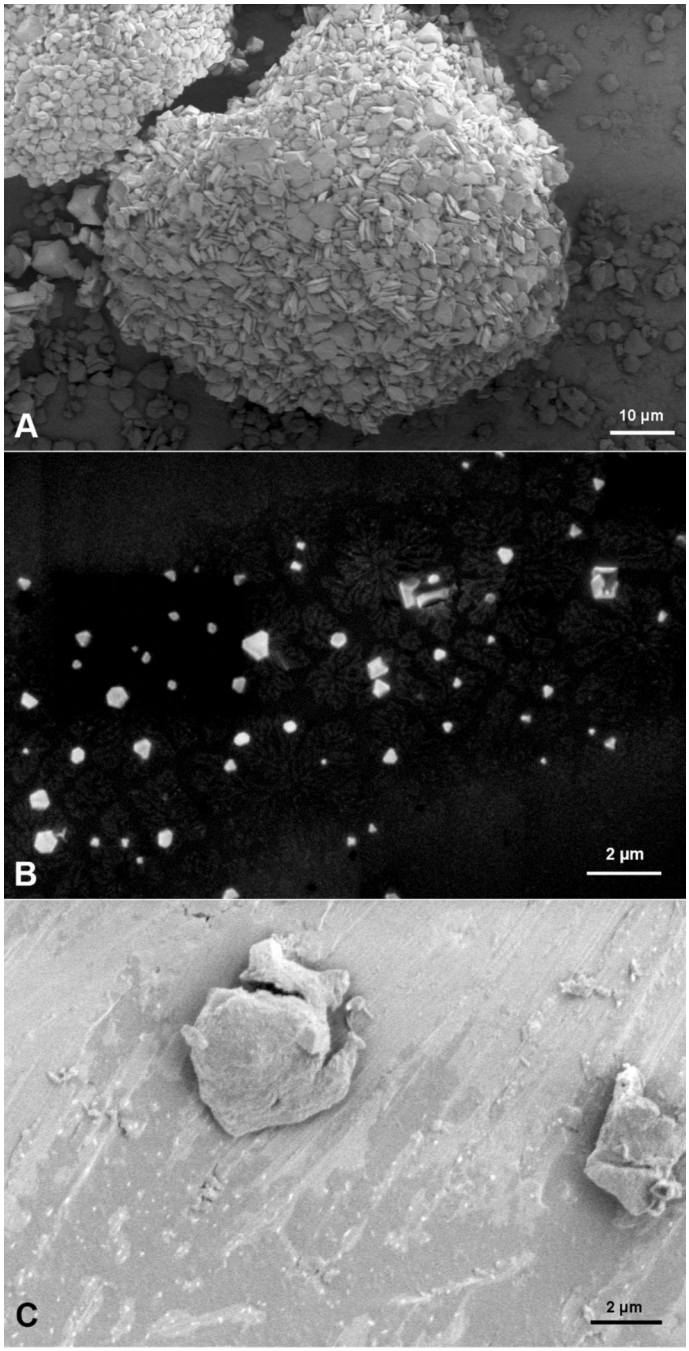

Figure 4.
SEM micrographs of insulin particles; (A) shows unprocessed insulin particles (scale bar 10 μm); (B) shows insulin nanoparticles (scale bar 2 μm); and (C) shows insulin microparticles after processing (scale bar 2 μm).

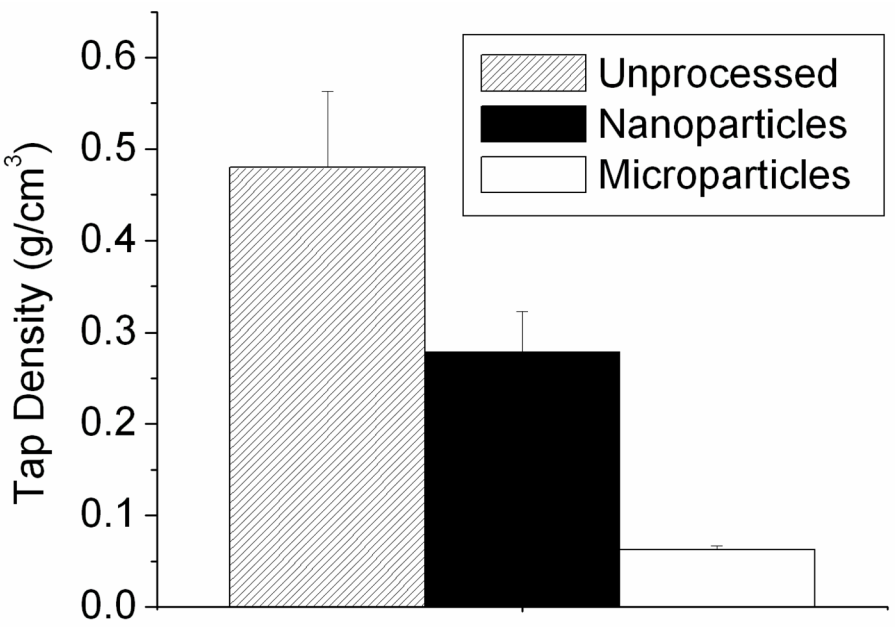

Figure 5.
Tap tests revealed the low density of insulin microparticle formulations. Each bar shows the mean ± S.D. of three experiments.

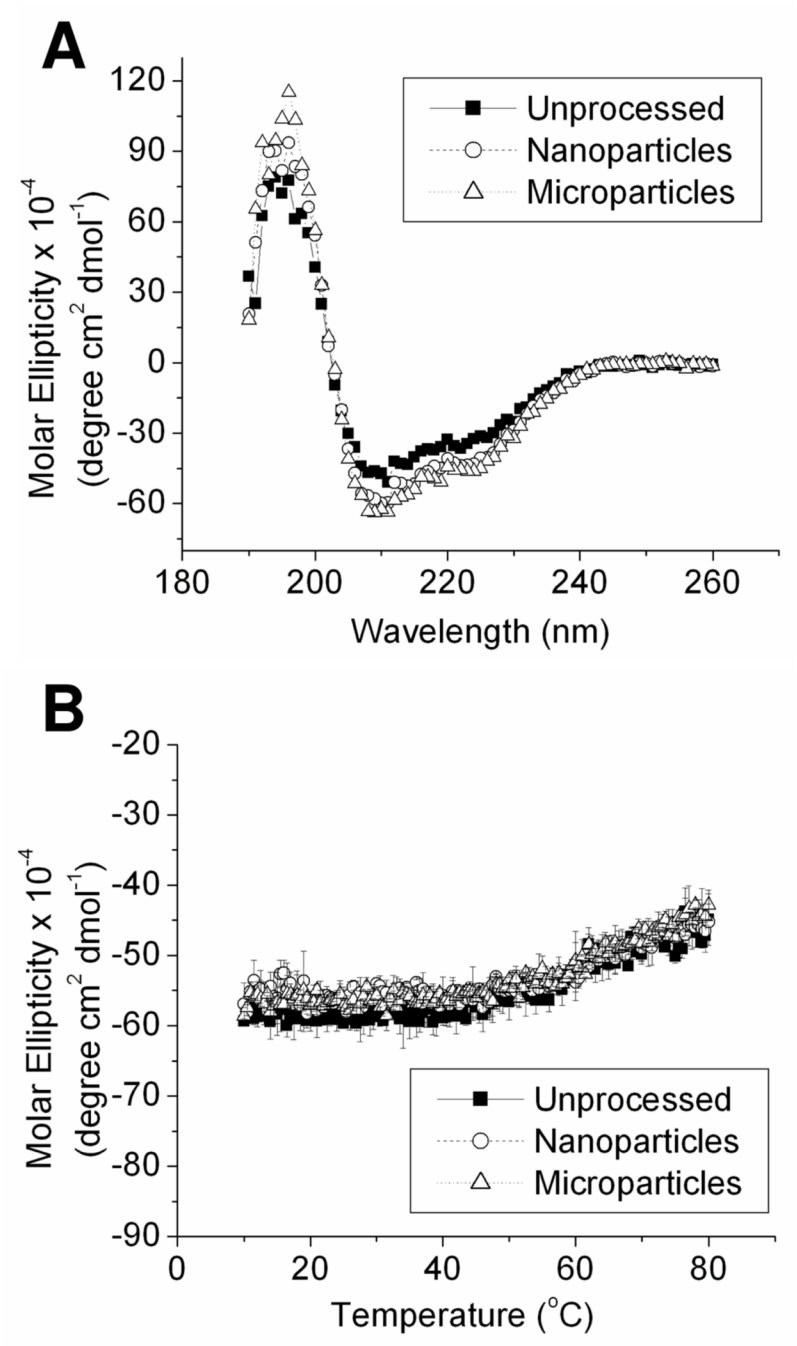

Figure 6.
Circular dichroism of dissolved insulin powders. Panel A shows isothermal spectra, and panel B shows variable temperature scans at a wavelength of 210 nm. Each value of the variable temperature scan represents the mean ± S.D. of three experiments.

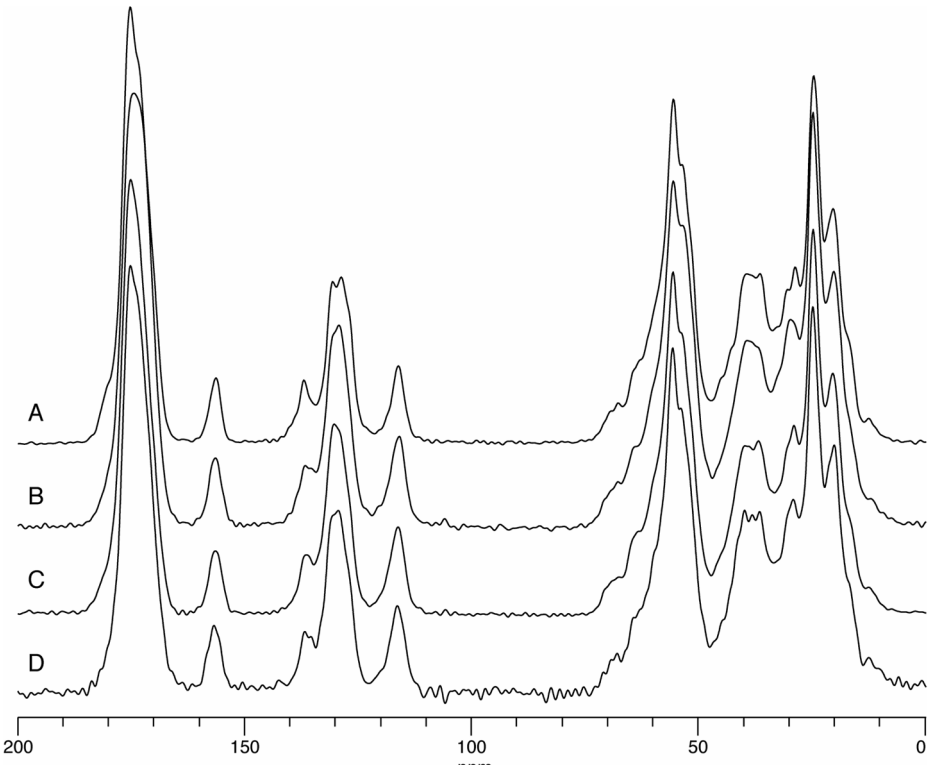

Figure 7.
13C CP/MAS NMR spectra for insulin powders; (A) Unprocessed; (B) Insulin microparticles; (C) Lyophilized insulin nanoparticles; (D) Centrifuged and dried insulin nanoparticles.

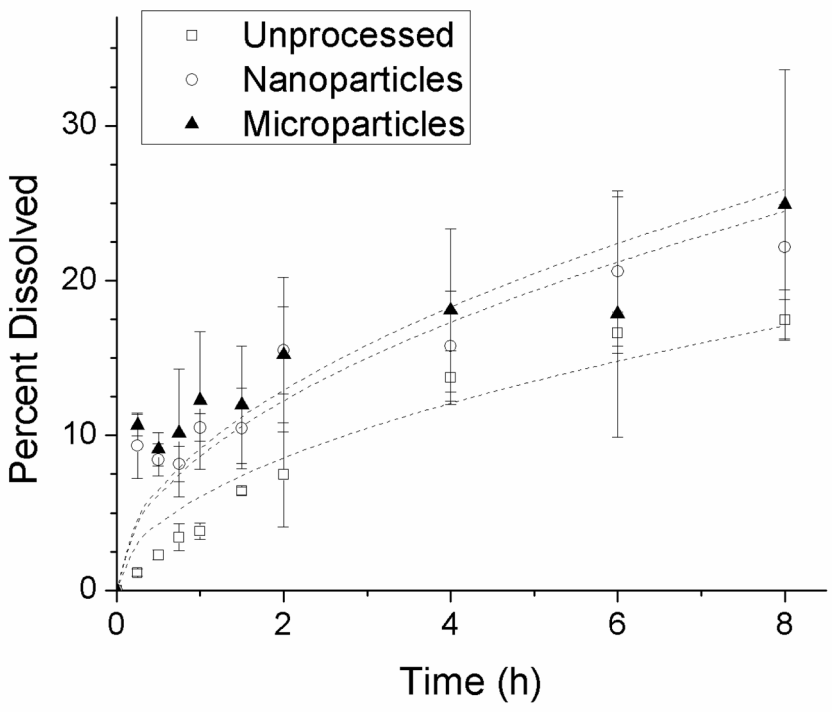

Figure 8.
Dissolution of insulin powders over time in phosphate buffered saline. Each point represents the mean ± S.D. of three experiments. Data were fit to the Higuchi equation (lines).

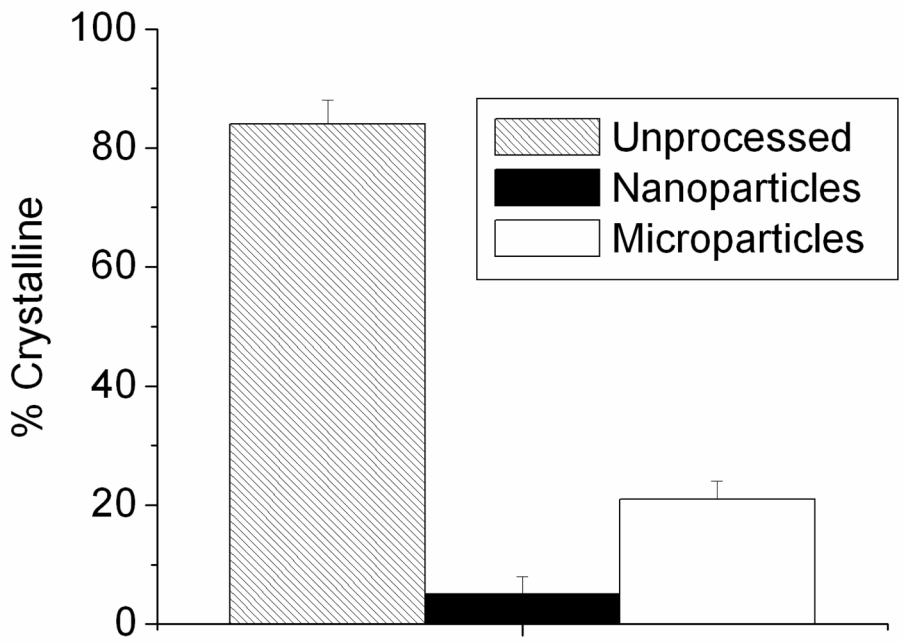

Figure 9.
The percent crystallinity of insulin particles, as determined by the HPLC dissolution method described in the U.S. Pharmacopeia and National Formulary. Each bar shows the mean ± S.D. of three experiments.

Table I

Characteristics of nanoparticles at various pH values.

pH	Diameter (nm)	Polydispersity	ζ-Potential (mV)
4.92	293 ± 42	0.38 ± 0.02	10.9 ± 2.4
4.97	345 ± 16	0.34 ± 0.02	15.6 ± 1.1
4.98	440 ± 58	0.36 ± 0.03	18.0 ± 1.3
5.09	592 ± 62	0.35 ± 0.01	17.6 ± 0.3

Table II

Particle sizes. Samples marked with an * were lyophilized and resuspended in aqueous solution before measuring their geometric diameters with a Coulter Counter.

Sample	d_{geo} (μm)	d_{aero} (μm)
Unprocessed*	12.0 ± 4.6	4.10 ± 1.8
Nanoparticles*	11.6 ± 9.5	3.60 ± 2.0
Microparticles	3.40 ± 1.4	2.30 ± 1.9